Pergamon

Geochimica et Cosmochimica Acta, Vol. 68, No. 16, pp. 3367–3377, 2004

0016-7037/04 $30.00 + .00

doi:10.1016/j.gca.2003.11.033

Oxygen isotope fractionation in synthetic magnesian calcite

Concepción Jiménez-López,[1,2,*] Christopher S. Romanek,[2,3] F. Javier Huertas,[1] Hiroshi Ohmoto,[4] and Emilia Caballero[1]

[1]Estacion Experimental del Zaidin, CSIC, Profesor Albareda 1, 18008 Granada, Spain
[2]Savannah River Ecology Laboratory, University of Georgia, Drawer E, Aiken, SC 29802, USA
[3]Department of Geology, University of Georgia, Athens, GA 30602, USA
[4]Astrobiology Research Center and Department of Geoscience, The Pennsylvania State University, University Park, PA 16802, USA

(*Received October* 16, 2002; *accepted in revised form November* 7, 2003)

Abstract—Mg-bearing calcite was precipitated at 25°C in closed system free-drift experiments from solutions containing $NaHCO_3$, $CaCl_2$ and $MgCl_2$. The chemical and isotope composition of the solution and precipitate were investigated during time course experiments of 24-h duration. Monohydrocalcite and calcite precipitated early in the experiments (<8 h), while Mg-calcite was the predominant precipitate (>95%) thereafter. Solid collected at the end of the experiments displayed compositional zoning from pure calcite in crystal cores to up to 23 mol% $MgCO_3$ in the rims. Smaller excursions in Mg were superimposed on this chemical record, which is characteristic of oscillatory zoning observed in synthetic and natural solid-solution carbonates of differing solubility. Magnesium also altered the predominant morphology of crystals over time from the {104} to {100} and {110} growth forms.

The oxygen isotope fractionation factor for the magnesian-calcite-water system (as $10^3\ln\alpha_{\text{Mg-cl-H}_2\text{O}}$) displayed a strong dependence on the mol% $MgCO_3$ in the solid phase, but quantification of the relationship was difficult due to the heterogeneous nature of the precipitate. Considering only the Mg-content and $\delta^{18}O$ values for the bulk solid, $10^3\ln\alpha_{\text{Mg-cl-H}_2\text{O}}$ increased at a rate of 0.17 ± 0.02 per mol% $MgCO_3$; this value is a factor of three higher than the single previous estimate (Tarutani T., Clayton R.N., and Mayeda T. K. (1969) The effect of polymorphims and magnesium substitution on oxygen isotope fractionation between calcium carbonate and water. *Geochim. Cosmochim. Acta* **33,** 987–996). Nevertheless, extrapolation of our relationship to the pure calcite end member yielded a value of 27.9 ± 0.02, which is similar in magnitude to published values for the calcite-water system. Although no kinetic effect was observed on $10^3\ln\alpha_{\text{Mg-cl-H}_2\text{O}}$ for precipitation rates that ranged from $10^{3.21}$ to $10^{4.60}$ μmol · m^{-2} · h^{-1}, it was impossible to disentangle the potential effect(s) of precipitation rate and Mg-content on $10^3\ln\alpha_{\text{Mg-cl-H}_2\text{O}}$ due to the heterogeneous nature of the solid.

The results of this study suggest that paleotemperatures inferred from the $\delta^{18}O$ values of high magnesian calcite (>10 mol% $MgCO_3$) may be significantly underestimated. Also, the results underscore the need for additional experiments to accurately characterize the effect of Mg coprecipitation on the isotope systematics of calcite from a chemically homogeneous precipitate or a heterogeneous material that is analyzed at the scale of chemical and isotopic zonation.

1. INTRODUCTION

Mg-calcite is an important mineral constituent of the skeletons of marine organisms (e.g., algae, brachiopods, mollusks, echinoderms; Lowenstam, 1961; Duplessy et al., 1970; Popp et al., 1986; Veizer et al., 1986; Brand, 1989; Rush and Chafetz, 1990; Carpenter and Lohman, 1995; Rahimpour-Bonab et al., 1997) and marine sedimentary cements (Gonzalez and Lohman, 1985; Carpenter et al., 1991; Saller and Moore, 1991). In addition, Mg-calcite has been used as a paleotemperature indicator, although there is debate as to whether it precipitates in isotope equilibrium with ambient water (Gonzalez and Lohman, 1985).

Mechanisms involving the incorporation of Mg in calcite and the effect of Mg on the properties of calcite have been the subject of intensive research and controversy for many years. Numerous studies have suggested that Mg inhibits calcite nucleation and growth (Lippmann, 1973; Reddy and Wang, 1980; Mucci and Morse, 1983, 1984; Deleuze and Brantley, 1997; Davis et al., 2000; Zhang and Dave, 2000). This inhibition is attributed to the higher activation energy (~20%) required for Mg^{2+} dehydration (compared to Ca^{2+}) on the surface of a growing crystal, which is the rate controlling step for the precipitation of carbonate from solution (Nancollas and Purdie, 1964).

Crystals grown from multicomponent aqueous solutions at relatively low temperature (e.g., 25°C) may display compositional gradients as a result of changes in the solid/liquid interface during crystal growth. Individual crystals may record the chemical or isotopic record of past crystallization events because once a layer is deposited, ionic solid state diffusion is negligible and previously formed layers tend not to reequilibrate with the solid/liquid interface (Prieto et al., 1997). To interpret these records, various factors must be considered such as kinetic effect, which potentially influence both the chemical and isotope systematics of the solid phase (Thortenson and Plummer, 1977; Berner, 1978; Lorens, 1981; Lahann and Siebert, 1982; Reeder and Grams, 1987). Physical expressions of kinetic effect have been documented in natural and synthetic carbonates. For instance, differences in chemical composition between sectors of a crystal were detected by Reeder and Prosky (1986) and Reeder and Paquette (1989), while intrasector zoning, which is a compositional zoning in time-equivalent

* Author to whom correspondence should be addressed, at Departamento de Microbiologia, Facultad de Ciencias, Universidad de Granada, Campus de Fuentenueva, 18071 Granada, Spain (cjl@ugr.es).

regions of a single sector, was observed by Paquette and Reeder (1990, 1995). Moreover, compositional zoning, and even oscillatory zoning, was observed within single sectors of synthetic barite crystals (Putnis et al., 1992) and (Ba,Sr)SO_4 and (Cd,Ca)CO_3 solid solutions (Prieto et al., 1997).

Less work has been conducted on isotope zoning in carbonate crystals. Dickson (1991) attributed variations in $\delta^{13}C$ and $\delta^{18}O$ values of concentric growth zones within coarsely crystalline inorganic calcite to variations in temperature and water composition during crystal growth. However, variations in $\delta^{13}C$ (~2‰) and $\delta^{18}O$ (~0.9‰) across different sectors of synchronously deposited material were attributed to differential kinetic isotope effect for distinct crystal faces.

Despite the abundance of Mg-calcite in nature and its importance in understanding sedimentary environments, including paleotemperatures, there is only one experimental study that quantified the effect of Mg incorporation on oxygen isotope partitioning in calcite. Tarutani et al. (1969) precipitated Mg-calcite from (Ca,Mg)$(HCO_3)_2$ solutions of different Mg-content. The solutions were initially saturated with $CO_{2(g)}$ and solid was precipitated in free-drift experiments by increasing the pH of the precipitating solution through the removal of aqueous CO_2 using a finely dispersed stream of $N_{2(g)}$. The bulk solid produced had a variable chemical content (4 to 12 mol% $MgCO_3$), depending on the initial composition of the solution. They concluded that Mg-calcite concentrated ^{18}O relative to pure calcite by 0.06‰ for each mol% $MgCO_3$ substituted in the crystal structure. This relationship does not generally complicate the interpretation of paleotemperatures from the $\delta^{18}O$ values of magnesian calcites. Nevertheless, Gonzalez and Lohmann (1985) showed that the $\delta^{18}O$ values of some magnesian calcites (>10 mol% $MgCO_3$) are not consistent with theoretical estimates based on the relationship reported by Tarutani et al. (1969). No other published data exist on the effect of Mg on the oxygen isotope systematics of Mg-calcite. In addition, no information exists on potential precipitation rate effects on oxygen isotope fractionation in systems containing Mg-calcite. Further, studies are lacking that quantify the effect(s) of the incorporation of Mg on carbon isotope partitioning in Mg-calcite (Jimenez Lopez et al., in review).

To evaluate the potential effect of Mg incorporation on the oxygen isotope systematics of calcite, time series experiments were conducted in which carbonate was precipitated in free-drift experiments from (Ca,Mg)Cl_2-$NaHCO_3$ solutions. The chemical composition of the solution was chosen to obtain Mg-calcite while minimizing the precipitation of aragonite and vaterite (Deleuze and Brantley, 1997). These solutions were periodically sampled over 24 h to monitor the chemical and isotope composition of the fluid and solid over time. The effect(s) of Mg and precipitation rate on the oxygen isotope fractionation factor (as $10^3 \ln\alpha$) for the magnesian-calcite-water system are reported below.

1. EXPERIMENTAL

2.1. Materials and Methods

Solutions containing $CaCl_2$ and $MgCl_2$ were mixed and added to aliquots of a $NaHCO_3$ solution that was preacidified with HCl to produce two groups of master solutions: 1) Group I: 0.32 mol/L $NaHCO_3$ + 0.0023 mol/L $CaCl_2$ + 0.00053 mol/L $MgCl_2$ and 2) Group II: 0.34 mol/L $NaHCO_3$ + 0.0023 mol/L $CaCl_2$ + 0.00105 mol/L $MgCl_2$. The initial Mg/(Mg + Ca) of the master solution ($X_{Mg,\ soln}$) was 0.19 for the Group I experiments and 0.31 for the Group II experiments.

Solid carbonate was precipitated from the master solutions using a modified version of the free drift technique, where the chemical composition of the solution drifted toward chemical equilibrium while pH was held relatively constant (see Jiménez-López et al., 2001, for details). The system was comprised of 18 cylindrical chambers that were each 7 × 14 cm in diameter. Four watch glasses (5 cm diameter each) containing master solution were placed inside each chamber on top of pedestals. Nucleation and growth of crystals was driven by the dissolution of $NH_{3(g)}$ into the master solution from an underlying reservoir of ammonium acetate (NH_4Ac) contained in each chamber. The hydrolysis of ammonia to $NH^+_{4(aq)}$ in the master solution raised and maintained solution pH at a near steady state value within 3 h of the initiation of an experiment.

Time step experiments were carried out at 25°C and 1 atm total pressure by placing the 18 chambers within a glove box. After purging the chambers and glove box with argon to exclude atmospheric CO_2, 10 mL aliquots of filtered (0.05 μm) master solution were loaded into each watch glass of a chamber. Ammonium acetate solution (100 mL) was then poured in the bottom of each chamber, and the chambers were securely fitted with lids, sealing each in a CO_2-free environment. The chambers were left to equilibrate for various lengths of time over the course of an experiment (24 h; see Table 1 for sampling intervals).

At specified time intervals, a single chamber was vented with argon. The solution from all four watch glasses was pooled, filtered (0.05 μm), and set aside for chemical and isotopic analysis. Solid was recovered from the filters and watch glasses, rinsed twice with distilled water and air dried at 40°C for 6 h. Chemical, isotopic and mineralogical analyses were performed on the solid. This experiment was replicated three times each for the Group I and Group II experiments.

2.2. Analyses

2.2.1. Chemical composition of solutions

At each sampling time point, pH and the concentration of total dissolved calcium ($Ca_{T(aq)}$), magnesium ($Mg_{T(aq)}$), and dissolved inorganic carbon (DIC) were determined. Solution pH was measured with a Cryson combination electrode. Concentrations of $Ca_{T(aq)}$ and $Mg_{T(aq)}$ were determined by atomic absorption spectrophotometry (AAS; Perkin-Elmer 1100B, using an air-acetylene flame atomizer) after the acidification of sample solutions with HCl to prevent the precipitation of carbonate. Analysis of DIC was carried out by acidimetric titration of 10 mL of filtered solution, using the Gran titration method (Stumm and Morgan, 1996). Based on the repeated analysis of standards and samples, the analytical uncertainly was ±0.05 for pH, ±0.01 mM for $Ca_{T(aq)}$ and $Mg_{T(aq)}$, and ±0.8 mM for DIC (reported as 1σ standard deviation in the text).

2.2.2. Mineralogical and Chemical composition of the solid

Solid material was analyzed by X-Ray diffraction (Philips PW 1730 diffractometer; 35 kV, 40 mA) to determine the mineralogy of the solid at each time step, using Al_2O_3 as an internal standard. The percentage of mineral phases in multimineralic mixtures was estimated from the peak area of the reflections for calcite (1 0 4), monohydrocalcite (0 1 2), aragonite (1 1 1), and vaterite (1 0 1) using calibration curves for mixtures of known mineralogical content (e.g., Davies and Hooper, 1963). Error in mineralogical composition was estimated at ±5%. The precipitate was also observed by optical microscopy to detect for the presence of amorphous phases, and samples were gold-coated and observed by scanning electronic microscopy (Zeiss DMS 950).

Calcium and magnesium content of the solid was analyzed by AAS after the dissolution of 1 mg of sample with 1 N HCl. Also, the Mg and Ca content of individual crystals was analyzed by EDX with a HR-TEM-AEM (Philips CM20; 200 kV, 56 μA). Crystals were embedded in resin and cut to 750 Å thickness for analysis. Collection time was 200 s for a 200 × 1000 Å window. Elemental transects were made along diagonals from the center to the vertex of a crystal. Olivine (25.37% Mg) and titanite (20.44% Ca) were used as internal standards for Mg and Ca, respectively. Experimental uncertainty associated with

Table 1. Chemical and mineralogical data for a representative Group I and Group II experiment; no shift was detected in calcite XRD pattern (revealing Mg incorporation in calcite structure) until 300 min for Group I and 180 min for Group II experiments.

	Solution					Solids							
Time (min)	pH	$Ca^{2+}_{T(aq)}$ (mM)	$Mg^{2+}_{T(aq)}$ (mM)	DIC (M)	$X_{Mg,\ soln}$	Mg-cl[a] (%)	Calcite (%)	Mhc[b] (%)	Aragonite (%)	Vaterite (%)	$(X_{Mg,\ solid})_{avg}$	$(X_{Mg,\ solid})_{inst}$	SA ($m^2 \cdot g^{-1}$)
Group I													
0	7.22	2.29	0.53	0.32	0.19								
15	8.06	1.76	0.53	0.34	0.23								
30	7.80	1.42	0.51	0.33	0.26								
45	8.15	0.88	0.53	0.31	0.38	0	0	100	0	0	0	0	
60	8.35	0.56	0.51	0.33	0.48	0	10	>80	<5	<5	0	0	
90	8.45	0.62	0.52	0.34	0.46	0	>65	30	0	<5	0	0	
120	8.58	0.41	0.48	0.32	0.54	0	>85	10	0	<5	0	0	
180	8.81	0.43	0.57	0.32	0.57	0	>90	5	0	<5	0	0	
300	9.00	0.40	0.51	0.30	0.56	>60	<30	5	0	<5	0.020	0.050	0.37
480	8.96	0.23	0.50	0.29	0.68	>95	0	0	0	<5	0.015	0.042	0.37
600	8.84	0.12	0.49	0.31	0.81	>95	0	0	0	<5	0.040	0.083	0.37
720	8.85	0.28	0.40	0.32	0.59	>95	0	0	0	<5	0.061	0.117	0.36
840	8.94	0.15	0.47	0.31	0.76	>95	0	0	0	<5	0.028	0.063	0.36
960	9.07	0.25	0.43	0.32	0.63	>95	0	0	0	<5	0.049	0.097	0.35
1080	9.13	0.11	0.47	0.30	0.82	>95	0	0	0	<5	0.040	0.083	0.35
1200	9.15	0.22	0.40	0.31	0.65	>95	0	0	0	<5	0.059	0.114	0.35
1320	9.09	0.25	0.43	0.29	0.63	>95	0	0	0	<5	0.047	0.094	0.35
1440	9.11	0.21	0.46	0.29	0.69	>95	0	0	0	<5	0.033	0.071	0.35
Group II													
0	7.24	2.29	1.05	0.34	0.31								
15	7.76	1.48	0.99	0.34	0.40								
30	8.09	0.94	1.00	0.33	0.52								
45	8.19	0.75	1.00	0.33	0.57								
60	8.24	0.66	1.00	0.33	0.60	0	0	>90	<5	<5	0	0	
90	8.38	0.43	1.00	0.33	0.70	0	>65	30	<5	0	0	0	
120	8.48	0.33	1.00	0.32	0.75	0	>85	<15	0	0	0	0	
180	8.61	0.34	0.95	0.33	0.73	40	50	5	<5	0	0.040	0.083	0.37
300	8.80	0.30	0.91	0.31	0.76	80	15	0	<5	0	0.060	0.115	0.37
480	8.90	0.18	0.89	0.30	0.83	>95	0	0	<5	0	0.070	0.132	0.37
600	8.96	0.34	0.80	0.28	0.70	>95	0	0	<5	0	0.109	0.195	0.37
720	9.02	0.32	0.80	0.29	0.71	>95	0	0	<5	0	0.110	0.197	0.36
840	9.00	0.29	0.79	0.30	0.73	>95	0	0	<5	0	0.130	0.229	0.36
960	9.07	0.18	0.83	0.30	0.82	>95	0	0	<5	0	0.091	0.165	0.35
1080	9.07	0.24	0.78	0.28	0.77	>95	0	0	<5	0	0.112	0.199	0.35
1200	9.15	0.19	0.83	0.29	0.81	>95	0	0	<5	0	0.091	0.166	0.35
1320	9.18	0.26	0.79	0.29	0.76	>95	0	0	<5	0	0.105	0.189	0.35
1440	9.16	0.21	0.78	0.29	0.79	>95	0	0	<5	0	0.110	0.198	0.35

[a] Mg-calcite.
[b] Monohydrocalcite.

these measurements was ±0.05 ppm from the repeated analysis of standards. More than 50 sections were prepared from crystals collected at the 60, 180, 960 and 1440 min time steps of an experiment.

The average value for the molar Mg content of the solid, $(X_{Mg,\ solid})_{avg}$, was calculated from the AAS measurement of the bulk solid. The Mg content of solid precipitated over a specific time step, $(X_{Mg,\ solid})_{inst}$, was calculated by difference between the Mg and Ca contents of the solution measured over two consecutive time intervals. Values of $(X_{Mg,\ solid})_{avg}$ were used with bulk isotope compositions to determine the relationship between Mg-content and oxygen isotope fractionation in the magnesian-calcite-water system, while $(X_{Mg,\ solid})_{inst}$ data were used to calculate the saturation state of the fluid with respect to a solid of particular [Mg/(Mg + Ca)] or $X_{Mg,\ solid}$ content.

2.2.3. *Isotope composition of solutions and solids and isotope fractionation factor*

The $\delta^{18}O$ value of solid carbonate ($\delta^{18}O_{solid}$) was determined according to procedures described in McCrea (1950) by analyzing the carbon dioxide produced by reacting 5 mg of solid with 2 mL of outgassed H_3PO_4 (100%) in an evacuated vessel at 25°C. The isotope composition of water ($\delta^{18}O_{H_2O}$) was measured at the beginning and end of each experiment using the technique described by Epstein and Mayeda (1953), by introducing a relatively small mass of carbon dioxide into 5 mL of sample solution isolated in a reaction vessel and allowing the mixture to equilibrate for 48 h in a thermostatic bath at 25°C before isotopic analysis.

All isotope measurements were made with an isotope ratio mass spectrometer (Finnigan MAT 251). Isotope ratios are expressed in conventional delta (δ) notation in per mil (‰) units (Craig, 1957). Delta values are calibrated against the V-PDB or V-SMOW international standard reference material using an in-house working standard (Reyes et al., 1989). Experimental uncertainty was ±0.1‰ for all measurements. The isotope fractionation factor for the magnesian-calcite-water system, calculated as $10^3 \ln\alpha_{Mg\text{-}cl\text{-}H_2O}$, was determined from $\delta^{18}O_{H_2O}$ and $\delta^{18}O_{solid}$ values measured after the 480 min time interval, when the solid was greater than 95% Mg-calcite.

2.2.4. *Saturation state and precipitation rate*

Saturation state with respect to Mg-calcite at any time interval was calculated by dividing the ionic activity product in solution (IAP) by

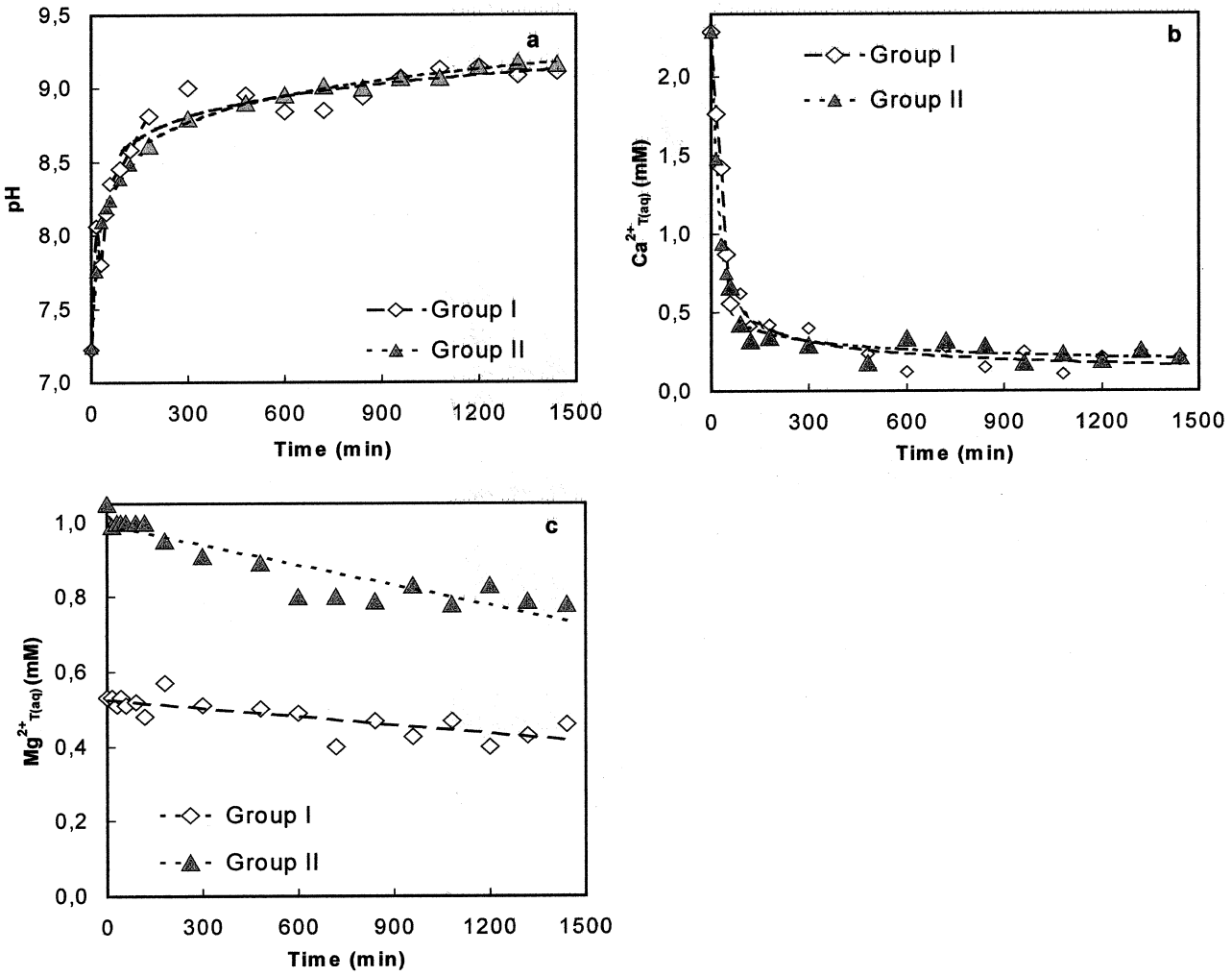

Fig. 1. Changes in the compositions of the master solution over time. (a) pH. (b) $Ca^{2+}_{T(aq)}$. (c) $Mg^{2+}_{T(aq)}$. Lines are the best fit of the experimental data points. Error bars are smaller than the size of the symbols used to represent the data here and in all subsequent plots where error bars are absent.

the solubility product for Mg-calcite (Busenberg and Plummer, 1989), considering the value of $(X_{Mg,\,solid})_{inst}$ for the solid over a particular time interval. IAP was calculated as the product of the activities (a) of calcium, magnesium and carbonate ions as $a(Ca^{2+})^{1-x} \cdot a(Mg^{2+})^{x} \cdot a(CO_3^{2-})$, where "x" is the mole fraction of Mg in the solution over a particular time interval (Mucci and Morse, 1983, 1984; Morse and Mackenzie, 1990). The activities for each ion were calculated with the EQPITZ program (He and Morse, 1993). The solubility product (K_{sp}) for a solid of particular $(X_{Mg,\,solid})_{inst}$ at any time during the time course experiment was calculated using the equation given by Busenberg and Plummer (1989; $A_0 = 6.27$ and $A_1 = 1.77$). Saturation state with respect to monohydrocalcite was calculated by dividing the IAP $[a(Ca^{2+}) \cdot a(CO_3^{2-})]$ by the solubility product for monohydrocalcite at 25°C ($10^{-7.6}$; Hull and Turnbull, 1973). Errors in saturation state with respect to Mg-calcite and monohydrocalcite were calculated from analytical errors in the determination of $Ca_{T(aq)}$, $Mg_{T(aq)}$, pH and DIC, and they were no greater than 20% for Mg-calcite and 10% for monohydrocalcite.

Mg-calcite precipitation rate was determined by dividing the mass of solid precipitated over a specified time interval (mass/time) by the average surface area of the cumulative seed material from the previous time steps. The mass of solid precipitated was calculated from calcium and magnesium consumption at each time interval. Surface area at a specific time interval was determined from the average length of the edge of the crystals observed in SEM photomicrographs and a geometrical model (for details, see Jiménez-López et al., 2001). Time intervals after 480 min were considered in these calculations because the solid was >95% Mg-calcite by this time step.

3. RESULTS

3.1. Chemical and Mineralogical Trends

Results from each of the three replicated runs for the Group I and II experiments showed little difference in measured values or trends over time. Therefore, the results from one representative run of each grouping are presented below.

3.1.1. Chemistry of solutions

The pH of the solution increased in the Group I and II experiments from an initial value of ~7.2 to ~9.1/9.2 at 1440 min (Fig. 1a; Table 1). This increase occurred primarily within the first 180 min of an experiment (~7.2 to ~8.6/8.8), after which time pH averaged 9.01 ± 0.11 (n = 10) for the Group I experiment and 9.03 ± 0.12 (n = 10) for the Group II exper-

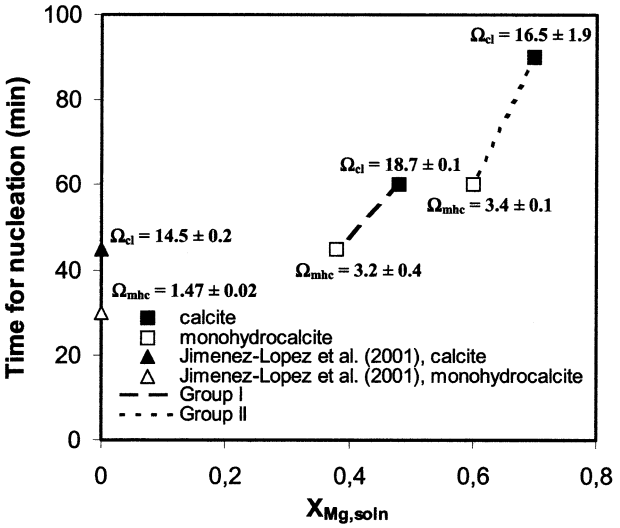

Fig. 2. Nucleation times for monohydrocalcite and calcite in Group I and Group II experiments. Data from Jiménez-López et al. (2001) are plotted for identical experiments in Mg-free solutions. Average and standard deviation values are calculated from saturation state data with respect to the relevant mineral phase at the time interval where monohydrocalcite or calcite crystals were first observed.

iment. There was no statistical difference in pH values between the two groupings after the 180 min time interval.

The concentration of $Ca_{T(aq)}$ fell from ~2.3 mM to ~0.2 mM during the time course experiment, with the decrease occurring rapidly during the first 180 min of an experiment (Fig. 1b; Table 1). The average value for $Ca_{T(aq)}$ after 180 min was 0.22 ± 0.09 mM (n = 10) and 0.25 ± 0.06 (n = 10) for the Group I and Group II experiments, respectively, with no statistical difference between the groupings.

The concentration of $Mg_{T(aq)}$ decreased from 0.53 mM to 0.46 mM in the Group I experiment, and from 1.05 mM to 0.78 mM in the Group II experiment (Fig. 1c; Table 1). Total magnesium in solution was fairly constant for the first 90 to 120 min of an experiment and decreased slowly and episodically thereafter. The mole fraction of Mg^{2+} in solution ($X_{Mg,\ soln}$) increased from 0.19 to 0.81 over the first 600 min for the Group I experiment, and from 0.31 to 0.83 over the first 480 min for the Group II experiment. After this, $X_{Mg,\ soln}$ fluctuated for the duration of an experiment (Table 1).

Total dissolved inorganic carbon in solution (DIC) decreased slowly over time from 0.32/0.34 mol/L to 0.29 mol/L in the two sets of experiments (Table 1).

3.1.2. *Mineralogy, Chemistry and Morphology of the solid*

Solid was first detected at 45 min for the Group I experiment and 60 min for the Group II experiment (Fig. 2). The first solid observed displayed a spherulitic texture, but it was subsequently replaced by well faceted crystals. Monohydrocalcite, aragonite and vaterite were the first minerals detected by XRD (Table 1), although the reflections for the latter two polymorphs were only slightly above background. Neither aragonite or vaterite were observed by optical microscopy, SEM or HRTEM in the solid recovered from any time step. Calcite was first detected by XRD at 60 min for the Group I experiment and 90 min for the Group II experiment. Monohydrocalcite dominated the mineralogy of the solid at 45 to 60 min, but after 300 min it was no longer detected by XRD, and calcite was the primary constituent of the precipitate, followed by Mg-calcite as the experiment progressed. The incorporation of Mg in calcite was confirmed by a shift in the (104) d-spacing for calcite in XRD patterns at ~300 min for the Group I experiment, and at ~180 min for the Group II experiment. Thereafter, the amount of Mg-calcite increased until it composed greater than 95% of the total solid after 480 min for both groupings.

The average mole fraction of Mg in the solid $(X_{Mg,\ solid})_{avg}$ increased from 0.02 at 300 min to 0.06 at 720 min for the Group I experiment; for the Group II experiment, the values increased from 0.04 at 180 min to 0.13 at 840 min. After these time intervals, $(X_{Mg,\ solid})_{avg}$ fluctuated until the end of an experiment (Table 1). The calculated mole fraction of Mg in the solid precipitated over a specific time step, $(X_{Mg,\ solid})_{inst}$, increased from 0.05 to 0.12 for the Group I experiment, and from 0.08 to 0.23 for the Group II experiment over the same time intervals.

Representative profiles of $(X_{Mg,\ solid})_{inst}$ for a crystal collected at the end of the Group I and Group II experiments are shown in Figure 3. HRTEM-AEM analyses were performed at 10 points for the Group I crystal and 18 points for the Group II crystal, along a line from the center of the crystal to a corner along a diagonal. Although Mg was detected in the cores of the crystals, the intensity of the (104) X-Ray peak for Mg-calcite was near the detection limit. The maximum value of $(X_{Mg,\ solid})_{inst}$ occurred at the outer corner of each crystal (last layer formed between 22 and 24 h), reaching a value of ~0.02 for the Group I experiment, and ~0.07 for the Group II experiment. The increase in $(X_{Mg,\ solid})_{inst}$ was not constant but showed fluctuations of ~0.005 for the Group I experiment and ~0.010 for the Group II experiment. Although the absolute values of $(X_{Mg,\ solid})_{inst}$ were different in the 50 samples analyzed, the overall trend of Mg-free cores and Mg-rich rims was observed in all the samples analyzed.

The morphology of the crystals also changed over time. Initially, well-faceted rhombohedral crystals of calcite of the {104} form were observed, but over time two of the edges of (104) faces were replaced by prismatic (110) and (100) faces (Fig. 4). The morphology of Mg-calcite crystals was identical in the Group I and Group II experiments, despite the differing initial magnesium concentration of the master solutions.

3.1.3. *Precipitation rate and saturation state*

Mg-calcite precipitation rates for the Group I experiment (from 480–1440 min) ranged from $10^{3.63}$ to $10^{4.60}$ $\mu mol \cdot m^{-2} \cdot h^{-1}$ for saturation states [with respect to the relevant $(X_{mg,\ solid})_{inst}$ of Mg-calcite] ranging from ~14 to ~31. For the Group II experiment, precipitation rates ranged from $10^{3.21}$ to $10^{4.19}$ $\mu mol \cdot m^{-2} \cdot h^{-1}$ for saturation states ranging from ~20 to ~36 (Table 2).

3.2. Oxygen Isotope Systematics

The oxygen isotope composition of the solid ranged from 18.5‰ to 21.2‰ for the Group I experiment, and from 18.7‰ to 22.1‰ for the Group II experiment (Table 2), with minima

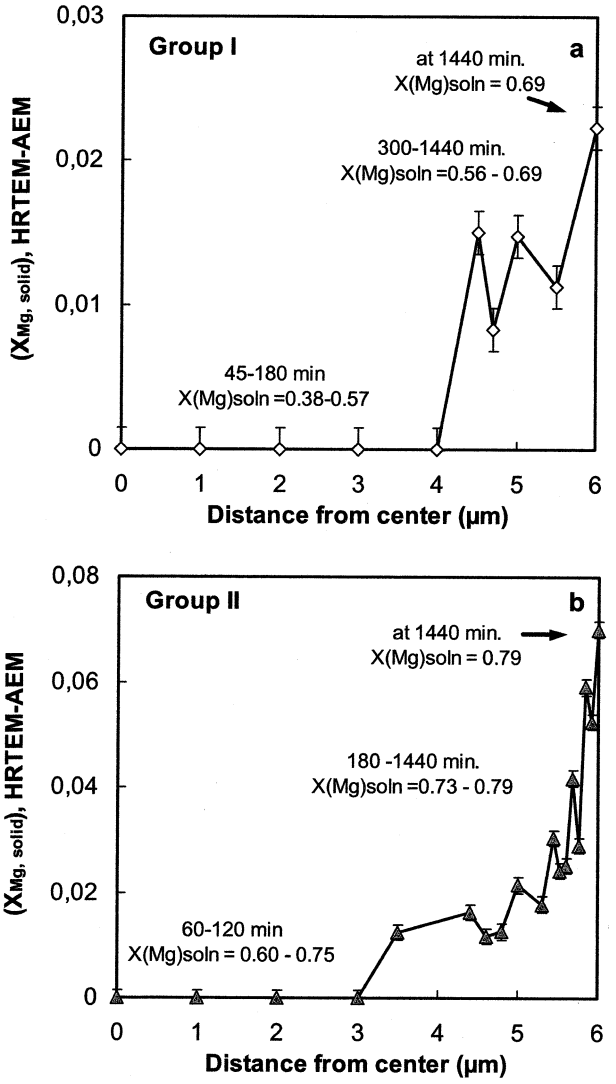

Fig. 3. Variation in $X_{Mg,\ solid}$ measured by HRTEM-AEM thin sections from the center of a crystal to a corner. Crystals were collected at 24 h time interval from (a) Group I and (b) Group II experiments.

observed at 60 min for both experiments (Fig. 5). The isotope composition of the water from which the solid precipitated averaged −8.2 ± 0.1‰, and it did not vary within or between experiments.

Over the time interval that Mg-calcite comprised greater than 95% of the solid (480 to 1440 min), $\delta^{18}O_{Mg\text{-}cl}$ values averaged 20.6 ± 0.3‰ (range: 20.2‰ to 21.2‰; n = 9) for the Group I experiment, and 21.8 ± 0.3‰ (range: 21.3‰ to 22.1‰; n = 8) for the Group II experiment (Fig. 5; Table 2). The oxygen isotope fractionation factor for the magnesian-calcite-H_2O system ($10^3\ln\alpha_{Mg\text{-}cl\text{-}H_2O}$) averaged 28.6 ± 0.3 (range: 28.2 to 29.2; n = 9) for the Group I experiment, and 29.8 ± 0.3 (range: 29.3 to 30.1; n = 8) for the Group II experiment (Table 2). The average $\delta^{18}O_{Mg\text{-}cl}$ and $10^3\ln\alpha_{Mg\text{-}cl\text{-}H_2O}$ values for the two groupings were significantly different at $p = 0.05$. Collectively, $10^3\ln\alpha_{Mg\text{-}cl\text{-}H_2O}$ values increased with $(X_{Mg,\ solid})_{avg}$ at a rate of 0.17 ± 0.02 per mol% $MgCO_3$ in the bulk solid ($r^2 = 0.8403$; Fig. 6a; Table 2). Values of $10^3\ln\alpha_{Mg\text{-}cl\text{-}H_2O}$ did not display any dependence on precipitation rate over a range of rates from $10^{3.21}$ to $10^{4.60}$ μmol · m^{-2} · h^{-1} (Fig. 6b).

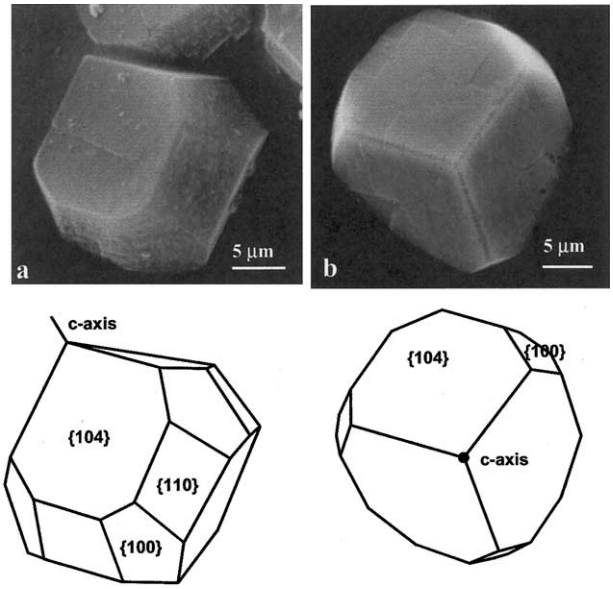

Fig. 4. SEM images and schematic drawings of crystals collected at the 24 h time interval in (a) Group I and (b) Group II experiments.

4. DISCUSSION

4.1. Effects of Mg on the Nucleation of Calcite and Monohydrocalcite

The time required for the nucleation of solid in the Group I experiment was 45 min for monohydrocalcite and 60 min for calcite, while for the Group II experiment, monohydrocalcite and calcite nucleated in 60 and 90 min, respectively. The increase in nucleation time at higher values of ($X_{Mg,\ soln}$) suggests that magnesium inhibited the formation of both minerals. This is consistent with the relatively short nucleation times observed by Jiménez-López et al. (2001) for pure calcite precipitated from Mg-free solutions in identical experiments.

Magnesium has been identified in synthetic and natural samples of monohydrocalcite (Brooks et al., 1950; Baron and Pesneau, 1956; Malone and Towe, 1970; Hull and Turnbull, 1973). In addition, several authors have discussed the inhibitory role of Mg in the nucleation of carbonates, especially calcite (Bischoff, 1968; Bischoff and Fyfe, 1968; Lippmann, 1973, Berner, 1975; Mucci and Morse, 1983; Deleuze and Brantley, 1997). The effect is probably related to the smaller size, higher charge density and greater hydration energy of Mg^{2+} compared to Ca^{2+} (Nancollas and Purdie, 1964; Lippmann, 1973; De Boer, 1977). Analogous effects have been attributed to the incorporation of Fe^{2+} in calcite (Meyer, 1984; Dromgoole and Walter, 1990a,b) and siderite (Jiménez-López and Romanek, 2004). As such, Mg probably inhibited monohydrocalcite nucleation in a fashion similar to that observed for calcite. Perhaps the presence of hydrated Ca- and Mg-bearing minerals in some carbonate bearing sediments is related to the relative rates of cation dehydration for Mg and Ca as well as the bulk chemistry of the associated fluids.

Table 2. Saturation state (Ω) of the master solution with respect to relevant mol% Mg-calcite, and Mg-calcite precipitation rate (r).[a]

Time (min)	$\Omega_{Mg\text{-}cl}$	log r (μmol · m^2 · h^{-1})	$\delta^{18}O_{solid}$ (‰)	$10^3\ln\alpha_{Mg\text{-}cl\text{-}H_2O}$
Group I				
0	6.0			
15	34.0			
30	15.3			
45	18.7		20.1	
60	18.6		18.5	
90	28.8		18.7	
120	19.7		19.8	
180	34.5		20.0	
300	32.9		20.3	
480	31.2	3.63	20.3	28.3
600	17.5	4.60	20.2	28.2
720	26.2	4.18	21.2	29.2
840	15.3	4.35	20.8	28.8
960	30.0	3.87	20.2	28.3
1080	14.3	4.39	20.9	28.8
1200	28.7	4.06	20.5	28.5
1320	29.0	—	20.7	28.7
1440	24.6	3.81	20.4	28.4
Group II				
0	6.7			
15	15.0			
30	18.7			
45	18.3			
60	17.8		18.7	
90	15.1		18.8	
120	13.2		19.1	
180	21.8		18.9	
300	23.5		—	
480	19.8	4.04	21.3	29.3
600	34.7	3.81	21.5	29.5
720	33.0	4.11	—	—
840	31.1	4.19	22.1	30.1
960	24.7	4.19	21.9	29.9
1080	29.6	3.21	22.0	30.0
1200	27.5	3.90	21.7	29.7
1320	36.0	3.92	22.1	30.1
1440	30.2	3.87	22.0	29.9

[a] Saturation calculations were made considering $(X_{Mg,\ solid})_{inst}$ for any time interval. Calculated oxygen isotope fractionation factor, as $10^3\ln\alpha_{Mg\text{-}cl\text{-}H_2O}$, for the magnesian-calcite-H_2O system was determined from the measured $\delta^{18}O_{solid}$ and a $\delta^{18}O_{H_2O}$ value of −8.2‰. A dash indicates that data are not available.

The presence of aqueous Mg also induced the precipitation of minimal amounts of aragonite and vaterite. These results are consistent with the observations of Lippmann (1973), Kitano and Kanamori (1966), Simkiss (1964), Berner (1975), Bischoff (1968) and Deleuze and Brantley (1997). Aragonite and vaterite probably formed because Mg adsorption and dehydration slowed the growth kinetics of calcite compared to the rates of formation for aragonite and vaterite. The relatively small size of Mg^{2+} cannot compensate for the electrical repulsion forces between neighboring CO_3^{2-} groups in the crystalline structure of aragonite or vaterite (Mucci and Morse, 1983). So, as the growth of aragonite and vaterite became inhibited by the adsorption of Mg onto the crystal surface, Mg-calcite was the only carbonate phase that continued to grow. Finally, Mg-calcite precipitation rates for this study are consistent with those of Mucci and Morse (1983) and Mucci (1986), when the data from these studies are extrapolated to the saturation state values of our experiments.

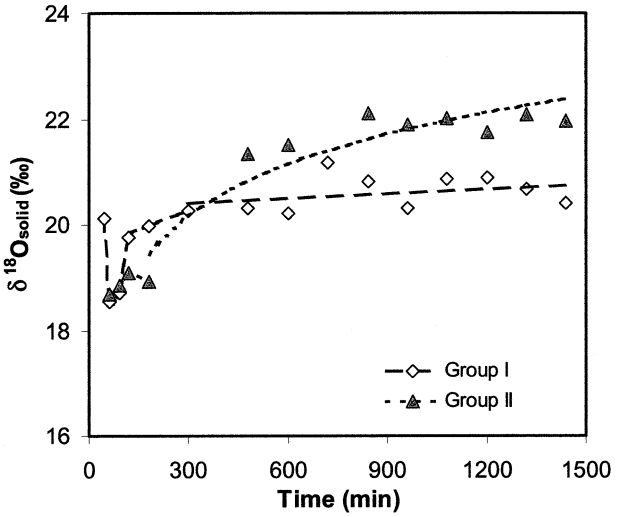

Fig. 5. Changes with time in the measured oxygen isotope composition of the solid ($\delta^{18}O_{solid}$). Lines are the best fit of the experimental data points.

4.2. Partition of Mg between Solution and Crystal

HRTEM-AEM measurements of Mg-calcite from the Group I and Group II experiments showed that $(X_{Mg,\ solid})_{inst}$ increased from the cores to the outer edges of the crystals (Fig. 3). The Mg-free cores can be explained by the fact that the incorporation of Ca in the crystal structure was kinetically favored compared to Mg. This is consistent with the AAS analyses of Ca from bulk samples collected during the early time steps of an experiment, and by the evolution of $Ca_{T(aq)}$ and $Mg_{T(aq)}$ over time. Because of the preferential incorporation of Ca in the solid, $Ca_{T(aq)}$ decreased relatively quickly (<120 min) in the master solution (Fig. 1b). Over this same time interval, $Mg_{T(aq)}$ was relatively constant (Fig. 1c), indicating Mg was not significantly incorporated in the solid. Magnesium eventually became a component of the precipitate and both aqueous Mg and Ca decreased in the later stages of an experiment. Finer scale excursions in the Mg-content of the solid can be attributed to an oscillatory zoning phenomenon, where the kinetics of heterogeneous nucleation and growth differ substantially for minerals that form solid solutions from end member compositions (e.g., $CaCO_3$ and $MgCO_3$) that have significantly different solubility products (Prieto et al., 1997). This phenomenon was expressed in complementary excursions of solution chemistry that occurred after 8 to 10 h of an experiment (see Fig. 1, Table 1).

Moreover, the adsorption of Mg onto distinct crystal faces produced a solid of changing morphology (Fig. 4). The adsorption of Mg^{2+} onto a growing face [e.g., (100) and (110)] slowed growth in these particular directions, permitting preferred growth forms to be expressed (Zhang and Dave, 2000). The differential adsorption of Mg onto nonequivalent faces was caused by differences in the concentration of potential-determining species within different sectors of a crystal (Lahann, 1978; Reeder and Paquette, 1989; Paquette and Reeder, 1995; Jiménez-López et al., 2003). This observation agrees with the sector zoning phenomenon described by Reeder and Prosky

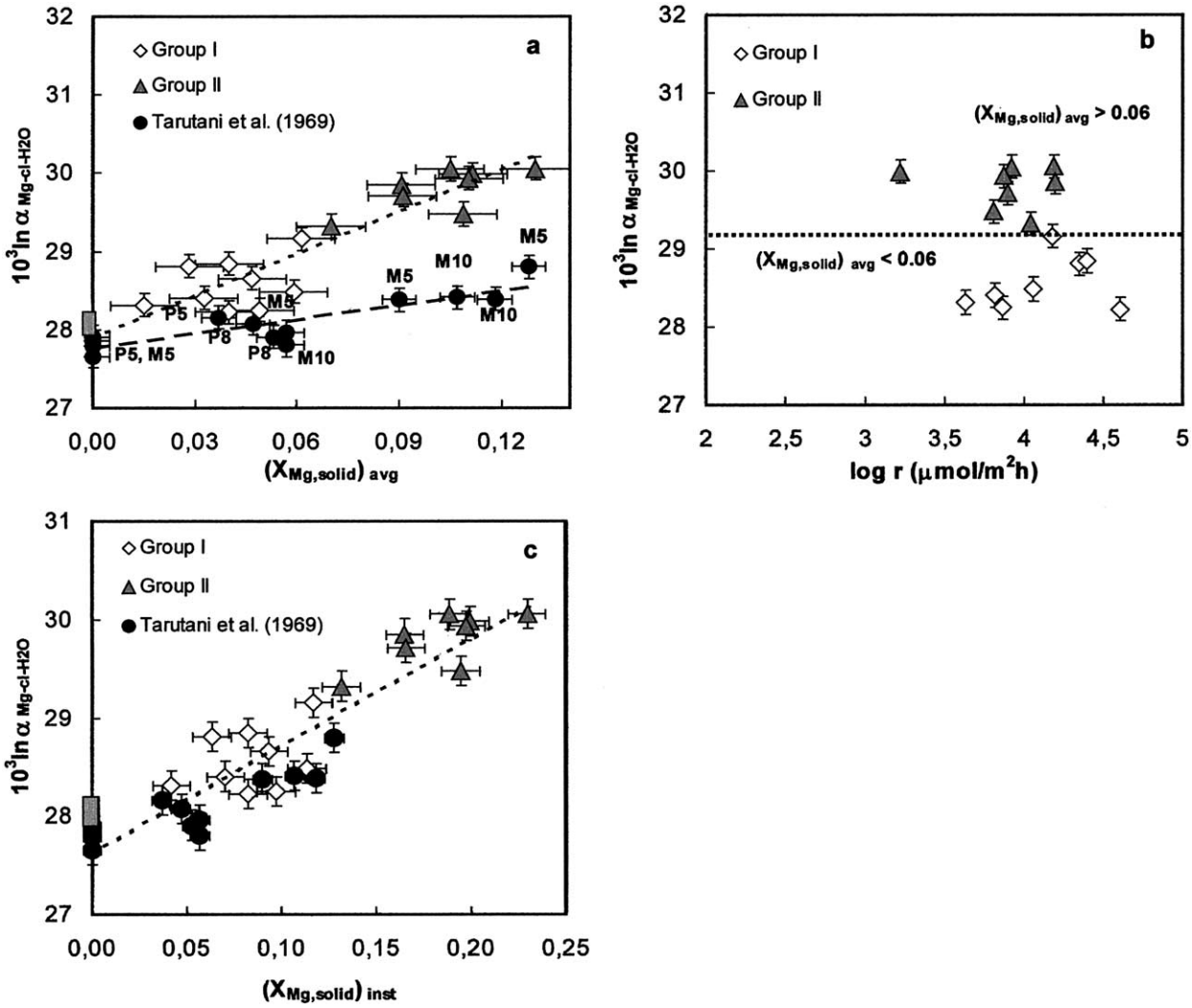

Fig. 6. Calculated oxygen isotope fractionation factors, as $10^3 \ln \alpha_{Mg\text{-}cl\text{-}H_2O}$, for the magnesian-calcite-H_2O system are plotted versus (a) $(X_{Mg,\,solid})_{avg}$, (b) precipitation rate, and (c) $(X_{Mg,\,solid})_{inst}$. Rectangles in (a) and (c) represent a range of published data from Epstein and Mayeda (1953), Bottinga (1968), O'Neil et al. (1969), Kim and O'Neil (1997) and Jiménez-López et al. (2001). The letters P and M followed by a number in (a) indicate the acids pyruvic (P) or malic (M) in g/L, used in the experiments of Tarutani et al. (1969).

(1986) and Reeder and Paquette (1989), who measured different chemical compositions for different sectors of $CaMg(CO_3)_2$ and Mg-calcite crystals.

Finally, the lack of agreement between the values of $(X_{Mg,\,solid})_{inst}$ determined by AAS and the HRTEM measurements can be explained by differences in the size of the sample populations and the spatial resolution afforded by the two analytical techniques. The bulk analysis of multiple grains by AAS provided an average Mg composition for specific time intervals over the time course experiment while the TEM analyses provided a spatially resolved analysis of two individual grains. In addition, the magnitude of the compositional gradient recorded by TEM (Fig. 3) depended highly on the particular sectors of the crystals that were chosen for the analysis. If the entire sample population of fifty grains analyzed by TEM were considered in the analysis, the mean of the distribution would approach that determined by the AAS analysis.

4.3. Influence of Mg on Oxygen Isotope Partitioning

Results from this study suggest that when calcite precipitates from solution of constant oxygen isotope composition, the $\delta^{18}O$ value increases with Mg-content at a rate of 0.17 ± 0.02‰ per mol% $MgCO_3$ in the bulk solid (Fig. 6a). The positive relationship observed here is consistent with the trend in $\delta^{18}O$ observed for Mg-calcite (Tarutani et al., 1969), for dolomite-calcite mineral pairs in high temperature experiments (Northrop and Clayton, 1966; O'Neil and Epstein, 1966), and dolomite-calcite mineral pairs in natural environments (Sheppard and Schwarcz, 1970). It is also consistent with theoretical considerations regarding the effect of cation substitution on oxygen isotope fractionation in carbonate minerals (O'Neil et al., 1969; O'Neil, 1986). However, the magnitude of the relationship is approximately three times greater than that reported by Tarutani et al. (1969). Whether the relationship observed

here represents a steady state condition or isotope equilibrium remains to be clarified through additional experimentation. Nevertheless, when the relationship is extrapolated to the pure calcite end member (i.e., the y-intercept), the calculated value of 27.9 ± 0.2 is similar to calcite-water fractionation factors, $10^3\ln\alpha_{\text{cl-H}_2\text{O}}$) reported in the literature (28.0 to 28.2: Epstein and Mayeda, 1953; Bottinga, 1968; O'Neil et al., 1969; O'Neil, 1986; Kim and O'Neil, 1997; Jiménez-López et al., 2001).

Two considerations may help to explain the difference between our results and those of Tarutani et al. (1969). First, Tarutani et al. (1969) introduced pyruvic and malic acid (5 to 10 g/L) to the solutions from which Mg-calcite precipitated. They reported that the acids decreased the $\delta^{18}O$ of pure calcite by ~0.3‰ compared to experiments lacking these constituents. The effect of organic acids on the oxygen isotope systematics of Mg-calcite is not known. Specific interaction effects between dissolved constituents and the solid may alter the $\delta^{18}O$ value of the solid directly, or the acids may contribute relatively ^{18}O-rich CO_2 to the pool of CO_2 liberated during the acid digestion of the solid for stable isotope analysis.

Alternatively, the difference may be attributed to the analytical techniques used to characterize the mol% $MgCO_3$ in the Mg-calcite of the two studies. In our study, the mol% $MgCO_3$ was determined from the acid dissolution of the bulk solid while in Tarutani et al. (1969), magnesium content was determined from the shift of the (104) *d*-spacing for calcite in XRD patterns. For the latter technique to accurately predict the bulk mol% $MgCO_3$ from a chemically heterogeneous solid, the target must be X-Ray transparent. X-Ray diffractometers (e.g., using Cu Kα irradiation generated at 35 kV and 40 mA) have depth ranges from a fraction of a micron to a few microns at best (Cullity, 1978; Rodríguez-Gallego, 1982), so structural variations buried in a crystal at greater than ~5 to 6 microns depth will be difficult to detect. Milliman et al. (1971) and Bischoff et al. (1983) measured the Mg content of biogenic Mg-calcite using XRD and wet chemical techniques (AAS), and concluded the XRD method yielded erroneous results due to, among other things, the heterogeneous distribution of Mg in the target calcite. The crystals grown in our study and that of Tarutani et al. (1969) were relatively large and chemically zoned because they were grown under free drift conditions. If the XRD analyses of Tarutani et al. (1969) were biased toward the outermost layers of the crystals, this would result in an overestimation of the Mg-content of a bulk sample.

A direct comparison of the AAS and XRD results from samples of this study was not possible because of limitations on the sample mass required for the stable isotope analysis. Nevertheless, a comparison can be made between $(X_{\text{Mg, solid}})_{\text{avg}}$ and $(X_{\text{Mg, solid}})_{\text{inst}}$ values of our study to determine the relationship between the Mg content of the bulk solid and the outermost layer of the solid at each time step of an experiment. The slope of the least squares linear fit of these two variables was 1.63 [$\Delta(X_{\text{Mg, solid}})_{\text{inst}}/(X_{\text{Mg, solid}})_{\text{avg}}$; $r^2 = 0.975$ for n = 17), implying that the outer most layer was more than one and a half times higher in Mg than the bulk solid.

If the values for the mol% $MgCO_3$ from Tarutani et al. (1969) represent only the outermost layer of the bulk solid, they are more similar to the $(X_{\text{Mg, solid}})_{\text{inst}}$ values reported in our study than the bulk Mg measurements of the solid ($\delta^{18}O$ values from both studies are reported as bulk measurements). The relationship between $(X_{\text{Mg, solid}})_{\text{inst}}$ and bulk $\delta^{18}O$ values from this study and the data from Tarutani et al. (1969) are plotted in Figure 6c for comparison; collectively, they form a statistically significant linear relationship having the form: $10^3\ln\alpha_{\text{Mg-cl-H}_2\text{O}} = 0.11\ (\pm 0.009)\ (X_{\text{Mg, solid}})_{\text{inst}} + 27.6\ (\pm 0.1)$ ($R^2 = 0.8532$ for n = 30). While the coherence of the combined data supports the conclusion that a significant Mg effect exists for the isotope systematics of Mg-calcite, the comparison of a bulk measure for $\delta^{18}O$ and an instantaneous measure for Mg-content is still dissatisfying. To accurately estimate the effect of Mg content on oxygen isotope fractionation in the calcite-water system, either a homogeneous solid must be precipitated in chemical and isotopic equilibrium or measurements of Mg and $\delta^{18}O$ must be made on a heterogeneous solid at the scale of the compositional zoning. Only hints of the true relationship can be gleaned from the analyses performed here. More research is needed using a variety of experimental and analytical techniques to accurately constrain the relationship between $\delta^{18}O$ and Mg-content for Mg-calcite.

Nevertheless, these results suggest that extreme care should be taken when interpreting paleotemperatures from the oxygen isotope records of magnesian calcite. Interpretations based on the analyses of low Mg-calcite (LMC: < 5 mol% $MgCO_3$) should not be affected by our results (e.g., Duplessy et al., 1970; Carpenter et al., 1991; Saller and Moore, 1991; Carpenter and Lohman, 1995; Rahimpour-Bonab et al., 1997), but paleotemperatures inferred from high magnesian calcite (HMC: > 10 mol% $MgCO_3$; e.g., Gonzalez and Lohman, 1985; Carpenter et al., 1991; Wilson and Opdyke, 1996; Rahimpour-Bonab et al., 1997) may be underestimated by 5 to 8°C. This observation was first recognized by Gonzalez and Lohman (1985), who questioned the accuracy of the Tarutani et al. (1969) estimate based on the oxygen stable isotope analysis of Holocene reefal carbonates. They showed that $\delta^{18}O$ values of Mg-calcite cements were enriched up to 1.9‰ relative to calcite equilibrium compositions, and they concluded the effect of Mg on the fractionation factor for Mg-calcite was underestimated.

Finally, $10^3\ln\alpha$ values for the Mg-calcite-water system showed no dependence on precipitation rate within a range of rates from $10^{3.21}$ to $10^{4.60}$ $\mu\text{mol} \cdot \text{m}^{-2} \cdot \text{h}^{-1}$. Unfortunately, the significance of this observation is also compromised because of the interrelated nature of precipitation rate and mol% $MgCO_3$ for the Mg-calcite precipitated in this study. Mucci and Morse (1983) showed that the rate constant for Mg-calcite precipitated in chemo-stat experiments increased as the mol% $MgCO_3$ decreased in the precipitate. We observed no relationship between precipitation rate and mol% $MgCO_3$, but unlike the experiments of Mucci and Morse (1983), our solid varied in Mg-content and $\delta^{18}O$ value over time.

No other quantitative data exist regarding potential rate effects on the $\delta^{18}O$ of Mg-calcite. The effect of precipitation rate on the oxygen isotope fractionation factor between solid carbonates and water remains controversial. McConnaughey (1989) sampled skeletal material from corals that grew at two different sites and reported a growth rate effect on the oxygen isotope composition of the coral. The $\delta^{18}O$ value of the skeletal carbonate, in this case aragonite, remained constant for growth rates ranging from 15 to 5 $\text{mm} \cdot \text{yr}^{-1}$, but it increased dramatically at lower rates. Also, Owen et al. (2002) concluded that seasonal variation in growth rate was a governing factor influ-

encing the $\delta^{18}O$ and $\delta^{13}C$ values of scallop shells. However, Tarutani et al. (1969) and Kim and O'Neil (1997) concluded that precipitation rate had little to no effect on the oxygen isotope fractionation factor of calcite.

Regarding carbon isotope partitioning between calcite and $CO_{2(g)}$, no rate effect was observed over an extended range of precipitation rates ($10^{3.0}$ and $10^{5.7}$ $\mu mol \cdot m^2 \cdot h^{-1}$) from either chemo-stat (Romanek et al., 1992) or free-drift experiments (Jiménez-López et al., 2001). While these results are consistent with the finding that precipitation rate does not affect isotope partitioning between Mg-calcite and H_2O (or CO_2), the range of rates investigated is relatively narrow compared to the range of rates observed in nature, especially the lower boundary of precipitation rates. The occurrence of carbonates with inexplicably high $\delta^{18}O$ and $\delta^{13}C$ values in nature (e.g., Turner, 1982) have yet to be reconciled within the framework of known fractionation factors that exist in the peer-reviewed literature.

Acknowledgments—D. Jiménez-López wishes to thank support from the MEC Grant Program from Spain (FP95 (DGICYT)) and from the U.S. Department of Energy to the University of Georgia Savannah River Ecology Laboratory (DE-FC09-96-SR18546). Romanek acknowledges support from NASA Astrobiology Institute. Ohmoto acknowledges support from NASA Astrobiology Institute [NCC2-1057] and National Science Foundation [EAR-9706279 & EAR0229556]. Thanks go to Rodríguez-Navarro for help in the discussion of crystal morphology and the schematics drawings of the SEM pictures. Thanks also to L. S. Paddock for editorial assistance, Rodríguez-Gallego, D. Cole and anonymous reviewers for their valuable comments.

Associate editor: D. R. Cole

REFERENCES

Baron G. and Pesneau M. (1956) Sur l'existence et un mode de preparation du monohydrate de carbonate de calcium. *Compt. Rend.* **243,** 1217–1219.

Berner R. A. (1975) The role of magnesium in the crystal growth of calcite and aragonite from sea water. *Geochim. Cosmochim. Acta* **39,** 489–504.

Berner R. A. (1978) Discussion: Equilibrium, kinetics and the precipitation of magnesian calcite from seawater. *Am. J. Sci.* **278,** 1475–1477.

Bischoff J. L. (1968) Kinetics of calcite nucleation: Magnesium inhibition and ionic strengh catalysis. *J. Geophys. Res.* **73,** 3315–3322.

Bischoff J. L. and Fyfe W. S. (1968) The aragonite-calcite transformation. *Am. J. Sci.* **266,** 65–79.

Bischoff W. D., Bishop F. C., and Mackenzie F. T. (1983) Biogenically produced magnesian calcite: inhomogeneities in chemical and physical-properties; comparison with synthetic phases. *Am. Mineral.* **68**(11-1)**,** 1183–1188.

Bottinga Y. (1968) Calculation of the fractionation factor for carbon and oxygen isotope exchange in the system calcite-carbon dioxide-water. *J. Phys. Chem. Geosci.* **172,** 181–190.

Brand U. (1989) Biogeochemistry of Late Paleozoic North American brachiopods and secular variations of seawater composition. *Biogeochem.* **7,** 159–193.

Brooks R., Clark L. M., and Thurston E. F. (1950) Calcium carbonate and its hydrates. *Phil. Trans. R. Soc. Lond. A* **243,** 145–167.

Busenberg E. and Plummer L. N. (1989) Thermodynamic of magnesian calcite solid-solutions at 25 °C and 1 atm total pressure. *Geochim. Cosmochim. Acta* **53,** 1189–1208.

Carpenter S. J., Lohmann K. C., Holden P., Walter L. M., Huston T. J., and Halliday A. N. (1991) $\delta^{18}O$ values, $^{87}S/^{86}Sr$ and Sr/Mg ratios of Late Devonian abiotic marine calcite: Implications for the composition of ancient seawater. *Geochim. Cosmochim. Acta* **55,** 1991–2010.

Carpenter S. J. and Lohmann K. C. (1995) $\delta^{18}O$ and $\delta^{13}C$ values of modern brachiopod shells. *Geochim. Cosmochim. Acta* **59,** 3749–3764.

Craig H. (1957) Isotopic standards for carbon and oxygen and correction factor for massspectrometric analysis of carbon dioxide. *Geochim. Cosmochim. Acta* **12,** 133–149.

Cullity B. D. (1978) Elements of X-ray Diffraction 2nd ed. Addison-Wesley.

Davies T. T. and Hooper P. R. (1963) The determination of the calcite: aragonite ratio in mollusc shells by X-ray diffraction. *Min. Mag.* **262,** 608–612.

Davis K. J., Dove P. M., and DeYoreo J. J. (2000) The role of Mg^{2+} as an impurity in calcite growth. *Science* **260,** 1134–1137.

De Boer R. B. (1977) Influence of seed crystals on the precipitation of calcite and aragonite. *Am. J. Sci.* **277,** 38–60.

Deleuze M. and Brantley S. (1997) Inhibition of calcite crystal growth by Mg^{2+} at 100°C and 100 bars: Influence of growth regime. *Geochim. Cosmochim. Acta* **7,** 1475–1485.

Dickson J. A. D. (1991) Disequilibrium carbon and oxygen isotope variations in natural calcite. *Nature* **353,** 842–844.

Dromgoole E. L. and Walter M. (1990a) Inhibition of calcite growth rates by Mn^{2+} in $CaCl_2$ solutions at 10, 25 and 50°C. *Geochim. Cosmochim. Acta* **54,** 2991–3000.

Dromgoole E. L. and Walter M. (1990b) Iron and manganese incorporation into calcite: Effects of growth kinetics, temperature and solution chemistry. *Chem. Geol.* **81,** 311–336.

Duplessy J. C., Lalou C., and Vinot A. C. (1970) Differential isotopic fractionation in benthic foraminifera and paleotemperatures reassessed. *Science* **168,** 250–251.

Epstein S. and Mayeda T. (1953) Variation of ^{18}O contents of water from natural sources. *Geochim. Cosmochim. Acta* **4,** 213–224.

Gonzalez L. A. and Lohmann K. C. (1985) Carbon and oxygen isotopic composition of holocene reefal carbonates. *Geology* **13,** 811–814.

He S. and Morse J. W. (1993) The carbonic acid system and calcite solubility in aqueous Na-K-Ca-Mg-Cl-SO_4 solutions from 0 to 90°C. *Geochim. Cosmochim. Acta* **57,** 3533–3554.

Hull H. and Turnbull A. G. (1973) A thermochemical study of monohydrocalcite. *Geochim. Cosmochim. Acta* **37,** 685–694.

Jiménez-López C., Caballero E., Huertas F. J., and Romanek C. S. (2001) Chemical, mineralogical and isotopic behavior and phase transformation during the precipitation of calcium carbonate minerals from intermediate ionic solution at 25°C. *Geochim. Cosmochim. Acta* **65,** 3219–3231.

Jiménez-López C., Rodriguez-Navarro A., Domínguez-Vera J. M., and García-Ruiz J. M. (2003) Kinetic and morphological study of calcite-lysozyme interaction. *Geochim. Cosmochim. Acta* **67,** 1667–1676.

Jimenez-Lopez C. and Romanek C. S. (2004) Precipitation kinetics and carbon isotope partitioning of inorganic siderite at 25°C and 1 atm. *Geochim. Cosmochim. Acta* **68**(3), 557–571.

Kim S. T. and O'Neil J. R. (1997) Equilibrium and nonequilibrium oxygen isotope effects in synthetic carbonates. *Geochim. Cosmochim. Acta* **61,** 3461–3475.

Kitano Y. and Kanamori N. (1966) Synthesis of magnesian calcite at low temperatures and pressures. *Geochem.J.* **1,** 1–10.

Lahann R. W. (1978) A chemical model for calcite crystal growth and morphology control. *Soc. Econ. Paleontol. Mineral.* **48,** 337–344.

Lahann R. W. and Siebert R. M. (1982) A kinetic model for distribution coefficients and application to Mg-calcites. *Geochim. Cosmochim. Acta* **46,** 2229–2237.

Lippmann F. (1973) Sedimentary carbonate minerals. In *Mineral, Rocks and Inorganic Materials*. Springer-Verlag. Berlin-Heidelberg, New York (eds. W. von Engelhardt, T. Hahn, R. Roy and P. J. Wyllie), pp 43–96.

Lorens R. B. (1981) Sr, Cd, Mn and Co distribution coefficients in calcite as a function of calcite precipitation rate. *Geochim. Cosmochim. Acta* **45,** 553–561.

Lowenstam H. (1961) Mineralogy, O^{18}/O^{16} ratios and strontium and magnesium content of recent and fossil brachiopods and their bearing on the history of the oceans. *J. Geol.* **69,** 241–260.

McConnaughey T. (1989) ^{13}C and ^{18}O isotopic disequilibrium in biological carbonates: I. Patterns. *Geochim. Cosmochim. Acta* **53,** 151–162.

McCrea J. M. (1950) On the isotopic chemistry of carbonates and a paleotemperature scale. *J. Chem. Phys.* **18,** 849–857.

Malone Ph.G. and Towe K. M. (1970) Microbial carbonate and phosphate precipitates from sea water cultures. *Mar. Geol.* **9,** 301–309.

Meyer H. J. (1984) The influence of impurities on the growth rate of calcite. *J. Cryst. Growth* **66,** 639–646.

Milliman J. D., Gastner M., and Müller J. (1971) Utilization of magnesium in coralline algae. *Geol. Soc. Am. Bull.* **82,** 573–580.

Morse J. W. and Mackenzie F. T. (1990) Geochemistry of Sedimentary Carbonates. Elsevier.

Mucci A. (1986) Growth kinetics and compositions of magnesian calcites overgrowths precipitates from seawater: Quantitative influence of orthophosphate ions. *Geochim. Cosmochim. Acta* **50,** 2255–2265.

Mucci A. and Morse J. W. (1983) The incorporation of $Mg^{2+}$and Sr^{2+}into calcite overgrowths: Influences of growth rate and solution composition. *Geochim. Cosmochim. Acta* **47,** 217–233.

Mucci A. and Morse J. W. (1984) The solubility of calcite in seawater solutions of various magnesium concentration, $I_t = 0.697$ m at 25 °C and one atmosphere total pressure. *Geochim. Cosmochim. Acta* **48,** 815–822.

Nancollas G. H. and Purdie N. (1964) The kinetics of crystal growth. *Q. Rev.* **18,** 1–20.

Northrop A. C. and Clayton R. N. (1966) Oxygen isotope fractionation in systems containing dolomite. *J. Geol.* **74,** 174–196.

O'Neil J. R. (1986) Theoretical and experimental aspects of isotopic fractionation. In *Stable Isotopes in High Temperature Geological Process. Reviews in Mineralogy* **16**. Mineralogical Society of America (eds. J. W. Valley, H. P. Taylor Jr., and J. R. O'Neil), pp. 1–41.

O'Neil J. R. and Epstein S. (1966) Oxygen isotope fractionation in the system dolomite-calcite-carbon dioxide. *Science* **152,** 198–201.

O'Neil J. R., Clayton R. N., and Mayeda T. K. (1969) Oxygen isotope fractionation in divalent metal carbonates. *J. Chem Phys.* **51,** 5547–5558.

Owen R., Kennedy H., and Richardson C. (2002) Isotopic partitioning between scallop shell calcite and seawater: Effect of shell growth rate. *Geochim. Cosmochim. Acta* **66,** 1727–1737.

Paquette J. and Reeder R. J. (1990) New type of compositional zoning in calcite: Insights into crystal-growth mechanisms. *Geology* **18,** 1244–1247.

Paquette J. and Reeder R. J. (1995) Relationship between surface structure, growth mechanism and trace elements incorporation in calcite. *Geochim. Cosmochim. Acta* **59,** 735–749.

Popp B. N., Anderson T. F., and Sandberg P. A. (1986) Brachiopods as indicators of original isotopic composition in some Paleozoic limestones. *Geol. Soc. Am. Bull.* **97,** 1262–1269.

Prieto M., Fernández-González A., Putnis A., and Fernández-Díaz L. (1997) Nucleation, growth and zoning phenomena in crystallizing $(Ba,Sr)CO_3$, $Ba(SO_4, CrO_4)$, $(Ba,Sr)SO_4$ and $(Cd,Ba)CO_3$ solid solutions from aqueous solutions. *Geochim. Cosmochim. Acta* **61,** 3383–3397.

Putnis A., Fernández-Díaz L., and Prieto M. (1992) Experimentally produced oscillatory zoning in the $(Ba,Sr)SO_4$ solid solution. *Nature* **358,** 743–745.

Rahimpour-Bonab H., Bone Y., and Moussavi-Harami R. (1997) Stable isotope aspects of modern molluscs, brachiopods, and marine cements from cool-water carbonates, Lacepede Shelf, South Australia. *Geochim. Cosmochim. Acta* **61,** 207–218.

Reddy M. M. and Wang K. K. (1980) Crystallization of calcium carbonate in the presence of metal ions. I. Inhibition by magnesium ion at pH 8.8 and 25°C. *J. Cryst. Growth* **50,** 470–480.

Reeder R. J. and Grams J. C. (1987) Sector zoning in calcite cements crystals: Implications for trace elements distribution in carbonates. *Geochim. Cosmochim. Acta* **51,** 187–194.

Reeder R. J. and Paquette J. (1989) Sector zoning in natural and synthetic calcites. *Sediment. Geol.* **65,** 239–247.

Reeder R. J. and Prosky J. L. (1986) Compositional sector zoning in dolomite. *J. Sediment. Petrol.* **56,** 237–247.

Reyes E., Linares J., Caballero E., Nuñez R., Delgado A., Figueruela G. (1989) Selección de un patrón interno para la determinación isotópica de carbono y oxígeno en carbonatos. In *III Congreso de Geoquímica de España*, Monografía 1. Rugart S. A. (ed. Cedex), pp. 13–19.

Rodríguez-Gallego M. (1982) La Difracción de los Rayos X. Alhambra.

Romanek C., Grossman E., and Morse J. (1992) Carbon isotopic fractionation in synthetic calcite, effects of temperature and precipitation rate. *Geochim. Cosmochim. Acta* **56,** 419–430.

Rush P. F. and Chafetz H. S. (1990) Fabric-retentive, non-luminescent brachiopods as indicators of original $\delta^{13}C$ and $\delta^{18}O$ composition: A test. *J. Sediment. Petrol.* **60,** 968–981.

Saller A. H. and Moore J. R. (1991) Geochemistry of meteoric calcite cements in some Pleistocene limestones. *Sedimentology* **38,** 601–621.

Sheppard S. M. and Schwarcz H. P. (1970) Fractionation of carbon and oxygen isotopes and magnesium between coexisting metamorphic calcite and dolomite. *Contrib. Mineral. Petr.* **26**(3)**,** 161–198.

Simkiss K. (1964) Variation in the crystallization form of calcium carbonate from artificial sea water. *Nature* **201,** 492–493.

Stumm W. and Morgan J. J. (1996) Aquatic Chemistry. Wiley Intercience.

Tarutani T., Clayton R. N., and Mayeda T. K. (1969) The effect of polymorphims and magnesium substitution on oxygen isotope fractionation between calcium carbonate and water. *Geochim. Cosmochim. Acta* **33,** 987–996.

Thortenson D. C. and Plummer L. N. (1977) Equilibrium criteria for two components solid reacting with fixed composition in an aqueous phase—Example: The magnesian calcites. *Am. J. Sci.* **277,** 1203–1223.

Turner J. V. (1982) Kinetic fractionation of carbon-13 during calcium carbonate precipitation. *Geochim. Cosmochim. Acta* **46,** 1183–1191.

Veizer J., Fritz P., and Jones B. (1986) Geochemistry of brachiopods: Oxygen and carbon isotopic records of Paleozoic oceans. *Geochim. Cosmochim. Acta* **50,** 1679–1696.

Wilson P. A. and Opdyke B. N. (1996) Equatorial sea-surface temperatures for the Maastrichtian revealed through remarkable preservation of metastable carbonate. *Geology* **24,** 555–558.

Zhang Y. and Dave R. A. (2000) Influence of Mg^{2+} on the kinetics of calcite precipitation and calcite crystal morphology. *Geochim. Cosmochim. Acta* **163,** 129–138.